# 3-D Sound Propagation and Acoustic Inversions in Shallow Water Oceans

Dr. Ying-Tsong Lin
Applied Ocean Physics and Engineering Department
Woods Hole Oceanographic Institution
Woods Hole, MA  02543
phone: (508) 289-2329     fax: (508) 457-2194     email: ytlin@whoi.edu

## LONG-TERM GOALS

Sound propagation in the areas of continental shelves is complicated due to many three-dimensional (3-D) oceanographic and marine geologic features, such as shelfbreak frontal systems, nonlinear internal gravity waves and topographic variability. The long-term goals of this project are targeted on understanding the 3-D sound propagation effects caused by these environmental factors, and also on applying the 3-D sound propagation physics to acoustic inversions.

## OBJECTIVES

Due to the horizontal inhomogeneity in the water column caused by shelfbreak frontal systems, nonlinear internal gravity waves and other physical oceanographic processes, horizontal refraction of sound occurs and produces significant 3-D acoustic propagation conditions. One of the objectives of this project is to develop an efficient and accurate 3-D sound propagation model (both theoretical and numerical models) for applications related to low-frequency sonar systems.

In addition to the 3-D sound propagation study, this project also has the investigation on the feasibility of two specific inversion techniques in the area of continental slopes: (a) source localization and (b) bottom geoacoustic inversions. This work requires a solid understanding on 3-D sound propagation, and it is closely connected to the first topic.

## APPROACH

The technical approaches employed in the first study (3-D sound propagation) include theoretical analysis, numerical computation and real data analysis. A 3-D normal mode method is used to study canonical environmental models of shelfbreak front systems and nonlinear internal wave ducts. The WHOI 3D Parabolic-Equation (PE) wave propagation model [1] and a vertical-mode horizontal-PE model of the Weinberg-Burridge formalism [2] are used to study sound propagation in real situations. The idea of normal mode back-propagation is implemented for the acoustic inversion work. A two-dimensional (2-D) approach is developed first, and then will be generalized for 3-D cases. Experimental data collected from recent work on the New Jersey shelf (SW06 [3]), the East China Sea (QPE [4]) and the South China Sea (ASIAEX [5] and NLIWI [6]) are analyzed with collaboration with experiment participants.

# Report Documentation Page

| 1. REPORT DATE **SEP 2011** | 2. REPORT TYPE | 3. DATES COVERED **00-00-2011 to 00-00-2011** |
|---|---|---|

| 4. TITLE AND SUBTITLE **3-D Sound Propagation and Acoustic Inversions in Shallow Water Oceans** | 5a. CONTRACT NUMBER |
|---|---|
| | 5b. GRANT NUMBER |
| | 5c. PROGRAM ELEMENT NUMBER |

| 6. AUTHOR(S) | 5d. PROJECT NUMBER |
|---|---|
| | 5e. TASK NUMBER |
| | 5f. WORK UNIT NUMBER |

| 7. PERFORMING ORGANIZATION NAME(S) AND ADDRESS(ES) **Woods Hole Oceanographic Institution,Department of Applied Ocean Physics and Engineering,Bigelow 211, MS 11,Woods Hole,MA,02543** | 8. PERFORMING ORGANIZATION REPORT NUMBER |
|---|---|

| 9. SPONSORING/MONITORING AGENCY NAME(S) AND ADDRESS(ES) | 10. SPONSOR/MONITOR'S ACRONYM(S) |
|---|---|
| | 11. SPONSOR/MONITOR'S REPORT NUMBER(S) |

| 12. DISTRIBUTION/AVAILABILITY STATEMENT **Approved for public release; distribution unlimited** |
|---|

| 13. SUPPLEMENTARY NOTES |
|---|

| 14. ABSTRACT |
|---|

| 15. SUBJECT TERMS |
|---|

| 16. SECURITY CLASSIFICATION OF: | | | 17. LIMITATION OF ABSTRACT | 18. NUMBER OF PAGES | 19a. NAME OF RESPONSIBLE PERSON |
|---|---|---|---|---|---|
| a. REPORT **unclassified** | b. ABSTRACT **unclassified** | c. THIS PAGE **unclassified** | **Same as Report (SAR)** | **12** | |

**WORK COMPLETED**

The tasks completed in the year are described below.

*1. 3D PE model development*

The WHOI 3D PE program has been modifed for parallel CPU and GPU computing. Also, a. grid size requirement is also derived using the sampling theory:

$$\text{DFT sampling theory} \begin{cases} k_{y\,max} = \pi/\Delta y, \Delta k_y = \pi/L_y \; (|y| \le L_y, |k_y| \le k_{y\,max}) \\ k_{z\,max} = \pi/\Delta z, \Delta k_z = \pi/L_z \; (|z| \le L_z, |k_z| \le k_{z\,max}) \\ k_{\theta\,max} = \pi/\Delta\theta, \Delta k_\theta = \pi/L_\theta \; (|\theta| \le L_\theta, |k_\theta| \le k_{\theta\,max}) \end{cases},$$

where $k_{y,z,\theta}$ are the wavenumbers along the transverse, vertical and angular axes. This relations are fundamental, and they actually govern the requirements for the model grid size. Consieder that the goal of sound propagation modeling is to resolve all of the arrivls less than a given arrival angle $|\zeta| \le \zeta_{max}$ with a requried angular resolution $\Delta\zeta_{min}$. From $\zeta_{max}$ we can find that the maximal wave-numbers need to be $k_{y,z\,max} \ge k_0\sin\zeta_{max}$ and $k_{\theta\,max} \ge k_0 r\sin\zeta_{max}$, or equivalently for $\Delta y$, $\Delta z$, and $\Delta\theta$:

$$\Delta y, \Delta z \le \left(\sin\zeta_{max}\right)^{-1}\lambda_0/2 \;\text{ and }\; \Delta\theta \le \left(r\,\sin\zeta_{max}\right)^{-1}\lambda_0/2.$$

On the other hand, from the requiement of angular resolution $\Delta\zeta_{min}$, we can find that the wavenumber increment $\Delta k_{y,z} \le k_0\cos\zeta\,\Delta\zeta_{min}$ and $\Delta k_\theta \le k_0\,(r\cos\zeta\,\Delta\zeta_{min} + \sin\zeta\,\Delta r)$, or equivalently for the apertures $L_y$, $L_z$ and $L_\theta$,

$$L_{y,z} \ge \left(\cos\zeta\,\Delta\zeta_{min}\right)^{-1}\lambda_0/2 \;\text{ and }\; L_\theta \ge \left(r\cos\zeta\,\Delta\zeta_{min} + \sin\zeta\,\Delta r\right)^{-1}\lambda_0/2.$$

From this analysis, one can see that in cylindrical PE the models resoultion is degrading as the range goes further. To overcome the problem, two improved model grids are suggested, as shown in Figure 1. The performance of different PE models is shown in Figure 2, and one can see that the Cartesian PE and the cylindrical PE with adaptive grids agree with each other very well on the solution plane. On the other hand, the coarse-grid cylindrical PE produces large errors due to the degration of the model resolution.

*2. 3-D sound propagation effects caused by topographic variability*

Two types of topographic features that will cause 3-D sound propagation effects are studied in the year. The first feature is the seafloor scours. Because the bottom scours often have strong directivity, propagating sound will be focused along the scouring direction due to the transverse gradient on the bottom depth. Also, the horizontal focusing will vary with the source position. Using the method of verical model and horizontal PE, a 3-D sound propagation model with the adabaitc mode assumption is built. This model has been applied for an SW06 example. The model clearly shows that due to the

seafloor scours in the New Jersey shelf area propagating sound can be focused, as shown in the upper panel of Figure 3. Two source positions are modeled in the example, and the resultant focusing patterns are slightly different. Although the effects of the seafloor scours are profound, they will be masked episodically by the presence of water column fluctuations, such as nonlinear internal waves. Twenty-two-days data are used, and a long time average is taken for removing the episodic fluctuations. The data shows about 5-dB intensification due to the horizontal focusing. The data-model comparison is shown in the lower panel of Figure 3, and has very good agreement.

The second bathymetric feature that will cause strong 3-D sound focusing is the submarine canyon. A realistic model has been implemented to model 3-D sound propagation in the North Mien-Hua canyon northeast of Taiwan, see Figure 4. Because of the concave bathymetry, the sound reflected the seafloor will be focused, as shown in the lower panel of Figure 4. This also provides a plaussible explanation for the intensified ship noise recorded at a hydrophone array during the QPE experiment.

*3. Whispering gallery modes in nonlinear internal wave ducts*

Using 3-D normal mode theory, general solutions of sound pressure field in a curved internal wave duct is found:

$$p(r,\theta,z) =$$

$$\sum_{m,n} C_{mn} \underbrace{\left[A_d \ e^{i\left(k^2(z)-\zeta_m^2\right)^{\frac{1}{2}}z} + A_u \ e^{-i\left(k^2(z)-\zeta_m^2\right)^{\frac{1}{2}}z}\right]}_{\text{vertical modes}} \times \underbrace{\left[B_{out} \ H^{(1)}_{\eta_{mn}}\left(\zeta_m r\right) + B_{in} \ H^{(2)}_{\eta_{mn}}\left(\zeta_m r\right)\right]}_{\text{radial modes}} \times e^{i\eta_{mn}\theta}$$

where

$$H^{(1)}_v(x) = J_v(x) + i\,Y_v(x)$$

$$H^{(2)}_v(x) = J_v(x) - i\,Y_v(x)$$

The field is decomposed into vertical and radial components. For each vertical mode, there is a set of radial modes, which is a form of Bessel functions descrbing the horizontal component of the field. Also, the radial modes can propagate along the wave front. Two types of modes are found. One is the whispering gallery modes formed by the sound energy trapped by the outter wave. The other is full bouncing mode generated by the sound energy bouncing between inner and outter waves.

An exmple of 50 Hz sound propagation in a curved nonlinear internal wave duct with 25 km curvature is shown in Figrue 5. The upper panel shows the vertical modal structure, and the lower panels are the radial modes associated with the second vertical mode. From the radial mode shape, one can see that the radial mode 1 is a whiserping gallery mode since it is formed by the sound energy trapped by the outter wave, resulting a single hump close to the outter boundary.

*4. Adapative normal mode back-propagation approach*

A variety of localization methods with normal mode theory have been established for localizing low frequency, broadband signals in a shallow water environment. Gauss-Markov inverse theory is employed in this paper to derive an adaptive back-propagation approach. Joining with the *maximum a*

*posteriori* mode filter, this approach is capable separating signals from noisy data and back-propagating them without significant influence from noise. Numerical simulations are presented to demonstrate the robustness and accuracy of the approach presented, along with comparisons to other methods. Applications to real data collected from the SW06 experiment are presented in Figure 6, and the effects of water column fluctuations with scales from nonlinear internal waves to shelfbreak front variability are observed.

**RESULTS**

An improved 3-D cylindrical PE model with consistent azimuthal resolution is developed. This cylindrical model can complement the 3-D Cartesian PE for a cylindrical-wave like field. (The 3-D Cartesian PE is not good for a cylindrical-wave like field because its PE approximation errors increase in greater azimuth.

Reaslitic models are implemented to study the bathymetric effects on 3-D sound refraction and focusing. Experimental data also demostrate significant, nonnegotiable 3-D effect. Specifically, the cancave seafloor of a submarine canyon can cause sound focusing, more than 10-dB intensificiation is expected. Study on the whispering gallery effect in curved internal wave ducts indeed provides a simple, but elegant, theoretical model to the problem.

Finally, an adaptive normal mode back-propagation approach for low-frequency broadband sound source localization in a shallow-water ocean is established. Gauss-Markov inverse theory is used in both mode filtering and back-propagation. This unifies the adaptive normal mode back-propagation approach. The method can smoothly adapt to the signal-to-noise ratio and ensure an optimal balance between robustness and accuracy.

**IMPACT/APPLICATIONS**

The potential relevance of this work to the Navy is on increasing the capability of Naval sonar systems in shallow water areas. The contributions of the effort on studying 3-D sound propagation effects will be on assessing the environment-induced acoustic impacts. In addition, the investigation of acoustic inversions directly relates to the Navy sonar operation.

**TRANSITIONS**

The 3-D sound propagation model has a potential for transition.

**RELATED PROJECTS**

Experimental data were collected from the ONR ASIAEX, SW06 and QPE projects. Also, collabration with Dr. Megan Ballard of ARL, UT at Austin is established for the study on the horizontal refraction of propagating sound due to seafloor scours.

**REFERENCES**

[1]   T. F. Duda, *Initial results from a Cartesian three-dimensional parabolic equation acoustical propagation code*, *WHOI Technical Report No. WHOI-2006-041*, Woods Hole Oceanographic Institution, Woods Hole, MA, 2006.

[2]  R. Burridge and H. Weinberg, "Horizontal rays and vertical modes," in *Wave Propagation and Underwater Acoustics*, ed. J. B. Keller & J. S. Papadakis, pp. 86-152, Berlin, German: Springer, 1977.

[3]  D. J. Tang, J. N. Moum, J. F. Lynch, P. Abbot, R. Chapman, P. H. Dahl, T. F. Duda, G. Gawarkiewicz, S. Glenn, J. A. Goff, H. Graber, J. Kemp, A. Maffei, J. D. Nash, and A. Newhall, "Shallow Water '06, A joint acoustic propagation/nonlinear internal wave physics experiment," *Oceanography*, vol. 20, pp. 156-167, 2007.

[4]  A.E. Newhall et al., "Acoustics and oceanographic observations collected during the QPE Experiment by Research Vessels OR1, OR2 and OR3 in the East China Sea in the Summer of 2009," *WHOI Technical Report No. WHOI-2010-06*, Woods Hole Oceanographic Institution, Woods Hole, MA, 2010.

[5]  A.E. Newhall et al., "Preliminary Acoustic and Oceanographic Observations s form the ASIAEX 2001 South China Sea Experiment," WHOI Technical Report No, WHOI-2001-12, Woods Hole Oceanographic Institution, Woods Hole, MA, 2001.

[6]  D. B. Reeder, T. F. Duda, and B. Ma., "Short-Range Acoustic Propagation Variability on a Shelf Area with Strong Nonlinear Internal Waves," Oceans'08 (Kobe) Conference Proceedings, IEEE, 2008.

## PUBLICATIONS

### 1. Peer refereed paper

*Submitted*

2011  **Y.-T. Lin** and J.F. Lynch, "Analytical study of the horizontal ducting of sound by an oceanic front over a slope," J. Acoustc. Soc. Am. Express Letters

2011  M.S. Ballard, **Y.-T. Lin** and J.F. Lynch, "Horizontal refraction of propagating sound due to seafloor scours over a range-dependent layered bottom on the New Jersey shelf," J. Acoustc. Soc. Am.

*Accepted with revision*

2011  **Y.-T. Lin**, A.E. Newhall and J.F. Lynch, "Low-frequency broadband sound source localization using an adaptive normal mode back-propagation approach in a shallow-water ocean," J. Acoustc. Soc. Am.

2011  A.E. Newhall, **Y.-T. Lin**, J.F. Lynch, M.F. Baumgartner, and G.G. Gawarkiewicz, "An acoustic normal mode approach for long distance passive localization of vocalizing sei whales on a continental shelf," J. Acoustc. Soc. Am.

2011  J.A. Colosi, T.F. Duda, **Y.-T. Lin**, J.F. Lynch, A.E. Newhall, and B.D. Cornuelle, "Observations of sound-speed fluctuations on the New Jersey continental shelf in the summer of 2006," J. Acoustc. Soc. Am.

2011  J.F. Lynch, C. Emerson, P.A. Abbot, G.G. Gawarkiewicz, A.E. Newhall, **Y.-T. Lin**, T.F. Duda, "Are azimuthal isotropy and alongshelf translational invariance found in low-frequency acoustic propagation along the New Jersey shelfbreak?" J. Acoust. Soc. Am.
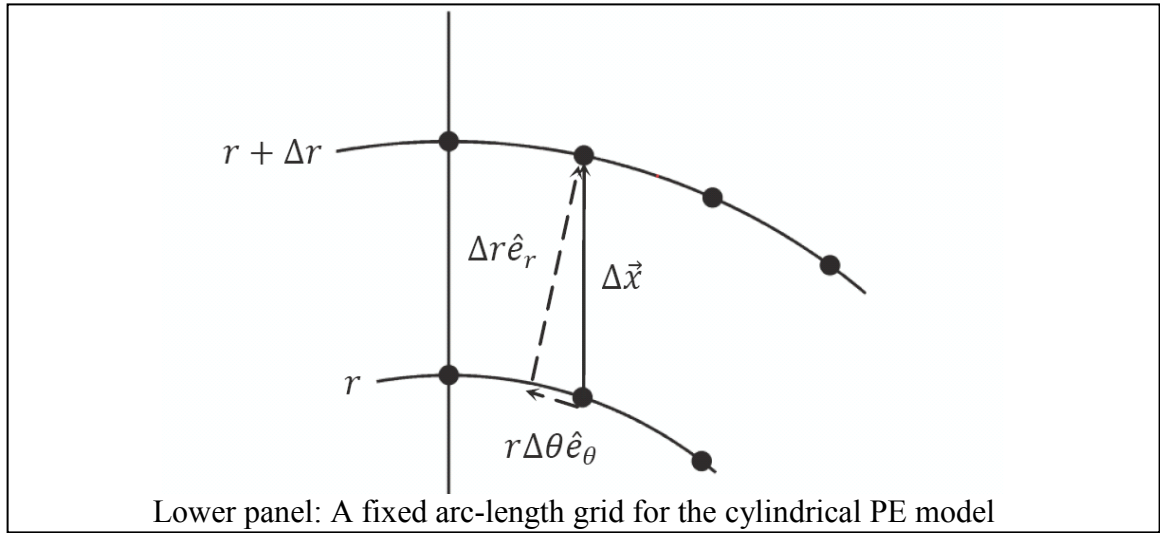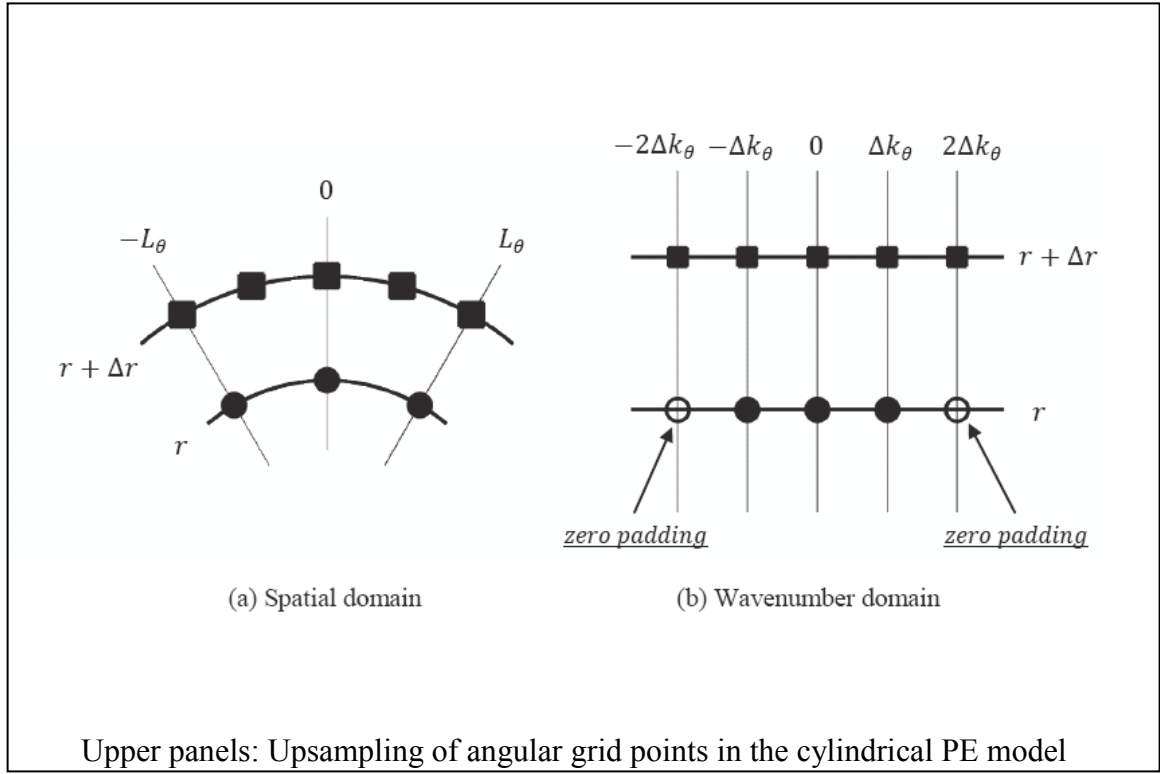
*In press*

2011 T.F. Duda, J.M. Collis, **Y.-T. Lin**, A.E. Newhall, J.F. Lynch, and H.A. DeFerrari, "Horizontal coherence of low-frequency fixed-path sound in a continental shelf region with internal-wave activity," J. Acoustc. Soc. Am.

*Published*

2011 T.F. Duda, **Y.-T. Lin**, and D.B. Reeder, "Observationally constrained modeling of sound in curved ocean internal waves: Examination of deep ducting and surface ducting at short range," J. Acoust. Soc. Am., vol. 130, pp. 1173-1187.

2011 L.Y.S. Chiu, **Y.-T. Lin**, C.-F.Chen, T.F. Duda, and B. Calder, "Focused sound from three-dimensional sound propagation effects over a submarine canyon,"J. Acoust. Soc. Am. Express Letters, vol. 129, pp. EL260-EL266.

2011 V.M. Kuz'kin, **Y.-T. Lin**, A.A. Lunkov, J.F. Lynch, and V.G. Petnikov, "Frequency shifts of the sound field interference pattern on oceanic shelf in summer conditions", Acoustical Physics, vol. 57, pp. 387-397.

2011 M. Badiey, B.G. Katsnelson, **Y.-T. Lin**, and J.F. Lynch, "Acoustic multipath arrivals in the horizontal plane due to approaching nonlinear internal waves", J. Acoust.Soc. Am. Express Letters, vol. 126, pp. EL141-EL147.

## 2. *First-author meeting proceeding and short abstract*

2011 **Y.-T. Lin**, W. G. Zhang, T. F. Duda, J. F. Lynch, and A. E. Newhall, "Study of underwater sound propagation in the continental shelf of the Mid Atlantic Bight with integrated physical oceanographic and acoustic models. (A)," J. Acoust. Soc. Am., vol. 129, pp. 2508.

2011 **Y.-T. Lin**, A. E. Newhall, T. F. Duda, and C.-F. Chen, "Numerical considerations for three-dimensional sound propagation modeling: coordinate systems and grid sizes," 10th International Conference on Theoretical and Computational Acoustics, Taipei, Taiwan, April 24-28, 2011.

2010 **Y.-T. Lin**, A. E. Newhall, and S. E. Parks, "Sound propagation modeling of right whale calls in Cape Cod Bay. (A)," J. Acoust. Soc. Am., vol. 128, pp. 2467.

2010 **Y.-T. Lin** and J. F. Lynch, "Low‐ frequency normal mode propagation in shallow water and its application to the acoustic inverse problem. (A)," J. Acoust. Soc. Am., vol. 128, pp. 2433.

(a) Spatial domain

(b) Wavenumber domain

Upper panels: Upsampling of angular grid points in the cylindrical PE model



Lower panel: A fixed arc-length grid for the cylindrical PE model

**Figure 1. Two improved model grids for the cylindrical PE model**

*[ Upper panels show the zero-padding on the wavenumber spectrum results in upsampling of angular grids. Lower panel shows the free propagation path occurred in a fixed arc-length grid.]*
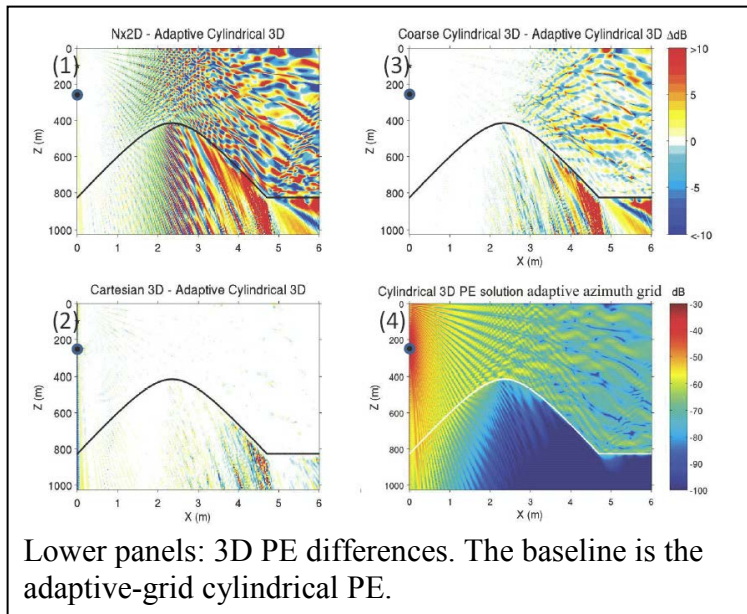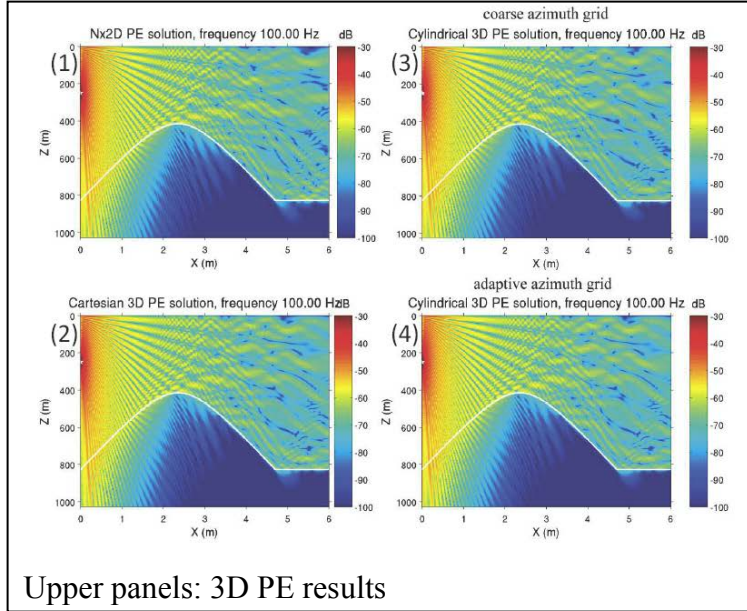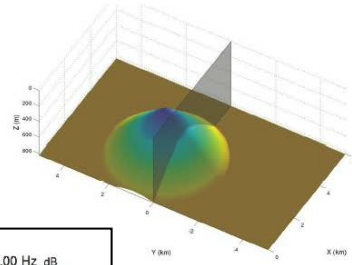
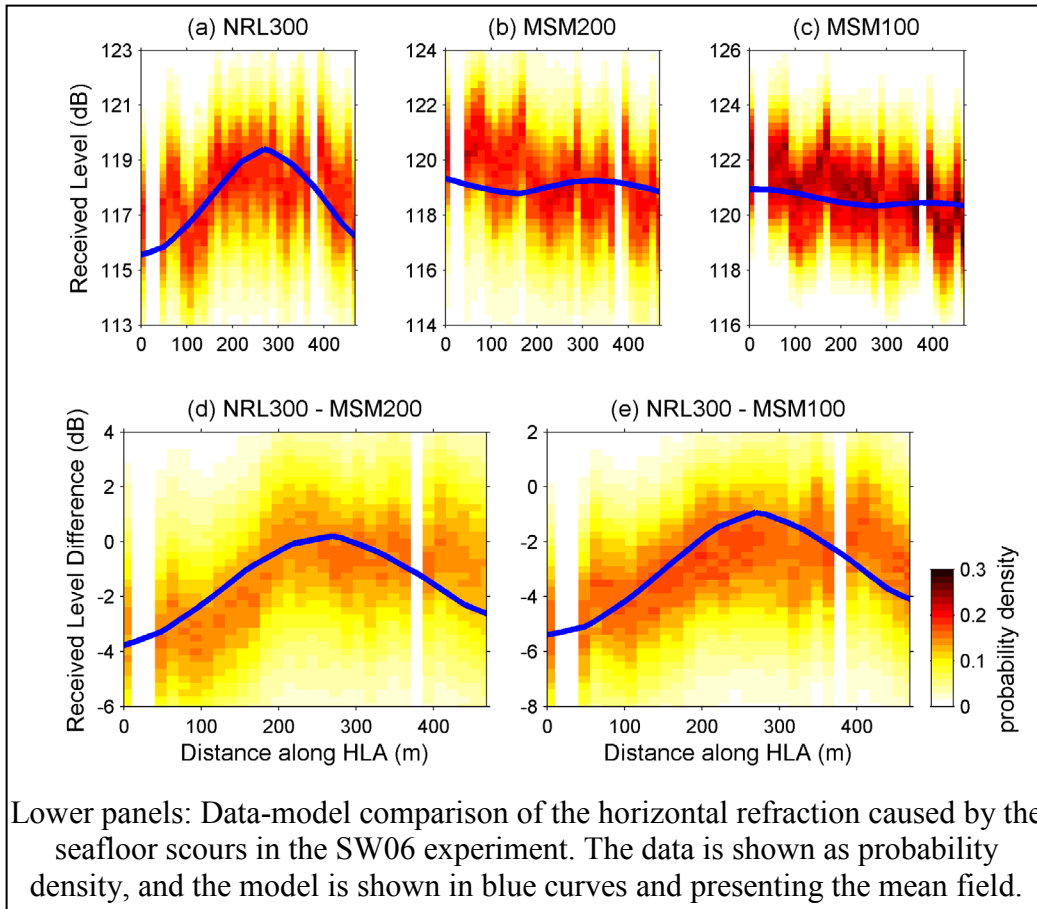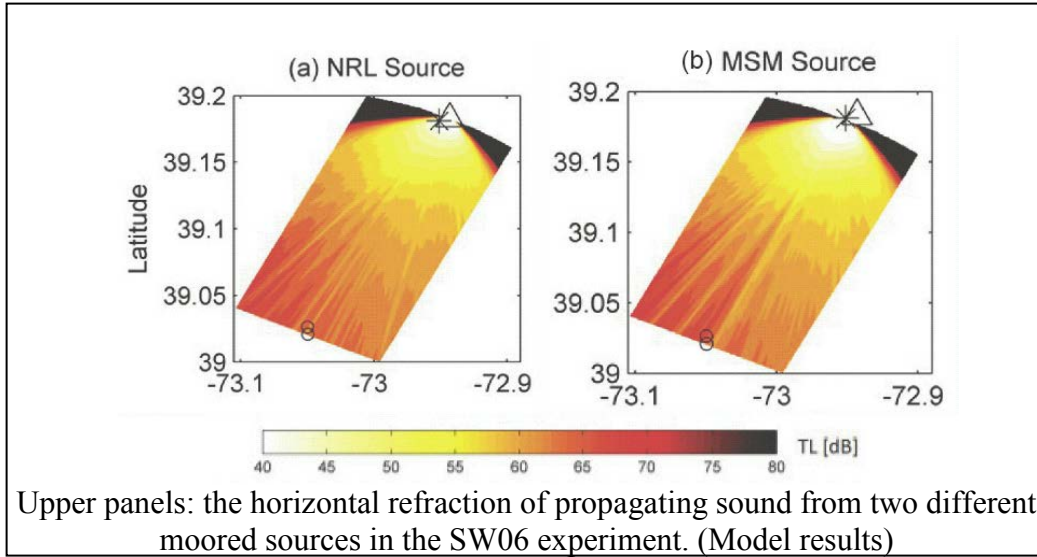# Modeling comparisons

Propagate over seamount, off center
Source at 250 m, 100Hz
4 cases – (1) Nx2D, (2) Cartesian, (3) coarse-grid
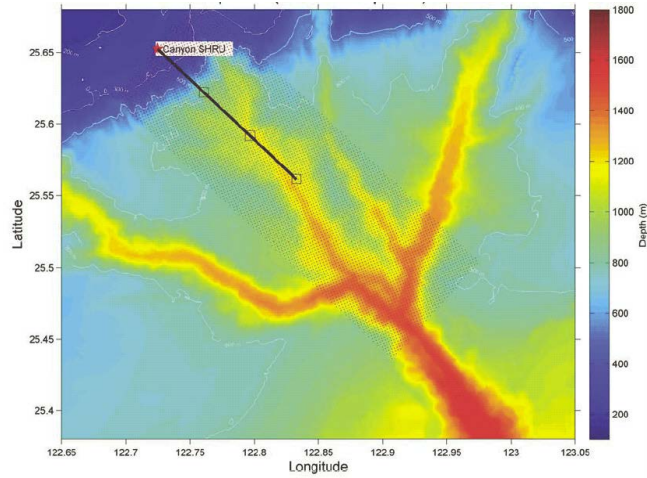cylindrical and (4) adaptive-grid cylindrical

Upper panels: 3D PE results

Lower panels: 3D PE differences. The baseline is the adaptive-grid cylindrical PE.

*Figure 2. PE model comparisons*

*[ Sound propagation over a seamount are computed by different 3D PE models, including (1) Nx2D (2) Cartesian, (3) coarse cylindrical grid and (4) adaptive cylindrical grid. The computed sound fields are shown in the upper panels, and the model differences are shown in the lower panels. The Cartesian PE and the cylindrical PE with an adaptive grid have very good agreement. ]*
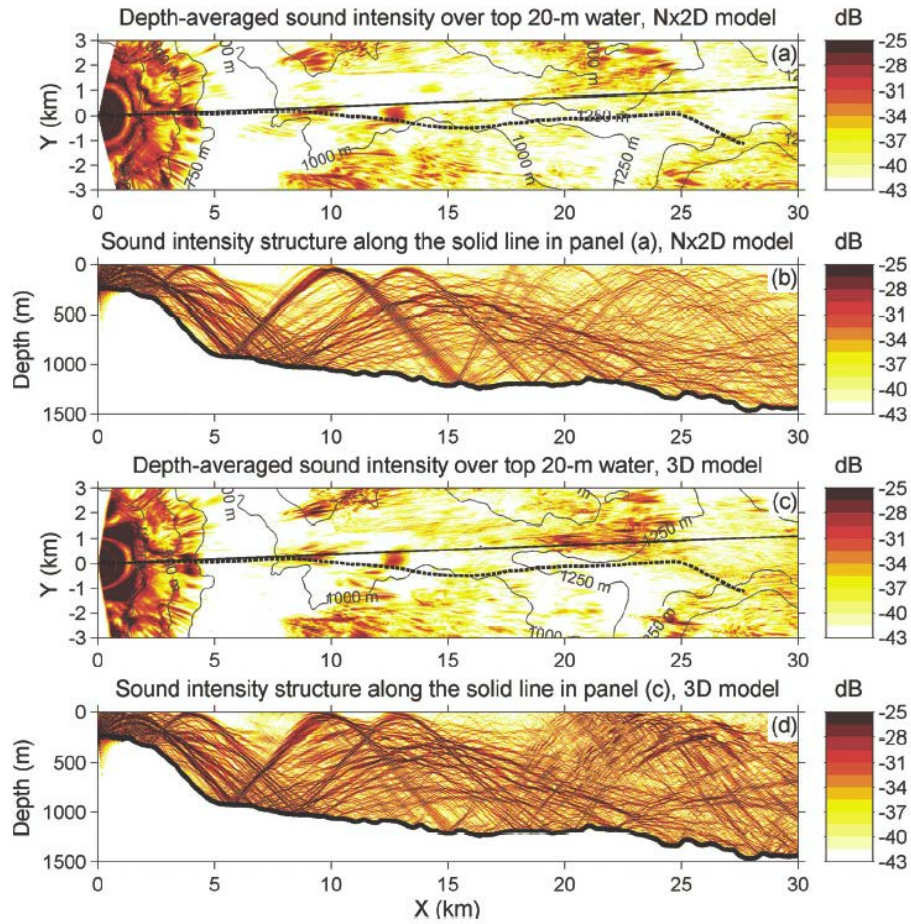
8

Upper panels: the horizontal refraction of propagating sound from two different moored sources in the SW06 experiment. (Model results)



Lower panels: Data-model comparison of the horizontal refraction caused by the seafloor scours in the SW06 experiment. The data is shown as probability density, and the model is shown in blue curves and presenting the mean field.

*Figure 3. Horizontal refraction of sound caused by seafloor scours*

*[ Acoustic data and models demonstrate the acoustic effect of seafloor scours on horizontal refraction. The model well captures the energy focus seen in the data. The sound frequencies are 100, 200 and 300 Hz. ]*
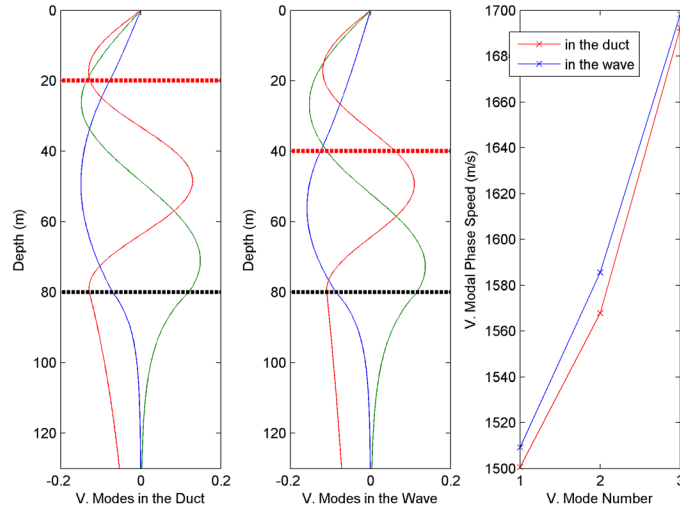
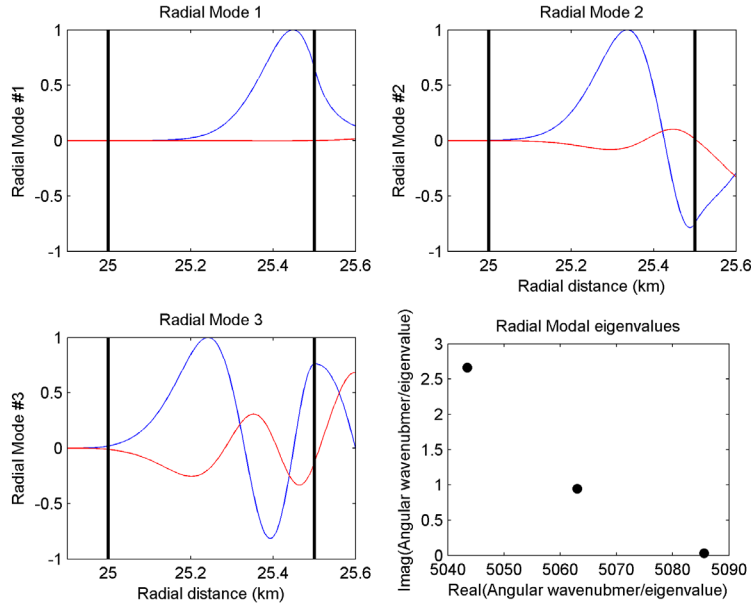(a) Bathymetry of the North Mien-Hua Canyon, northeast of Taiwan



(b) Comparison of Nx2D and 3D PE models. Acoustic frequency 300 Hz.

*Figure 4. Modeling of sound propagation over a submarine canyon*

*[ The bathymetry of the canyon system is shown in the panel (a), and the PE models are shown in panel (b). From the differences between the Nx2D and 3D PE's, one can see that the canyon bathymetry causes very strong sound focusing. The cylindrical spreading loss is removed in the plots to reduce the dynamic range of the TL variability. ]*

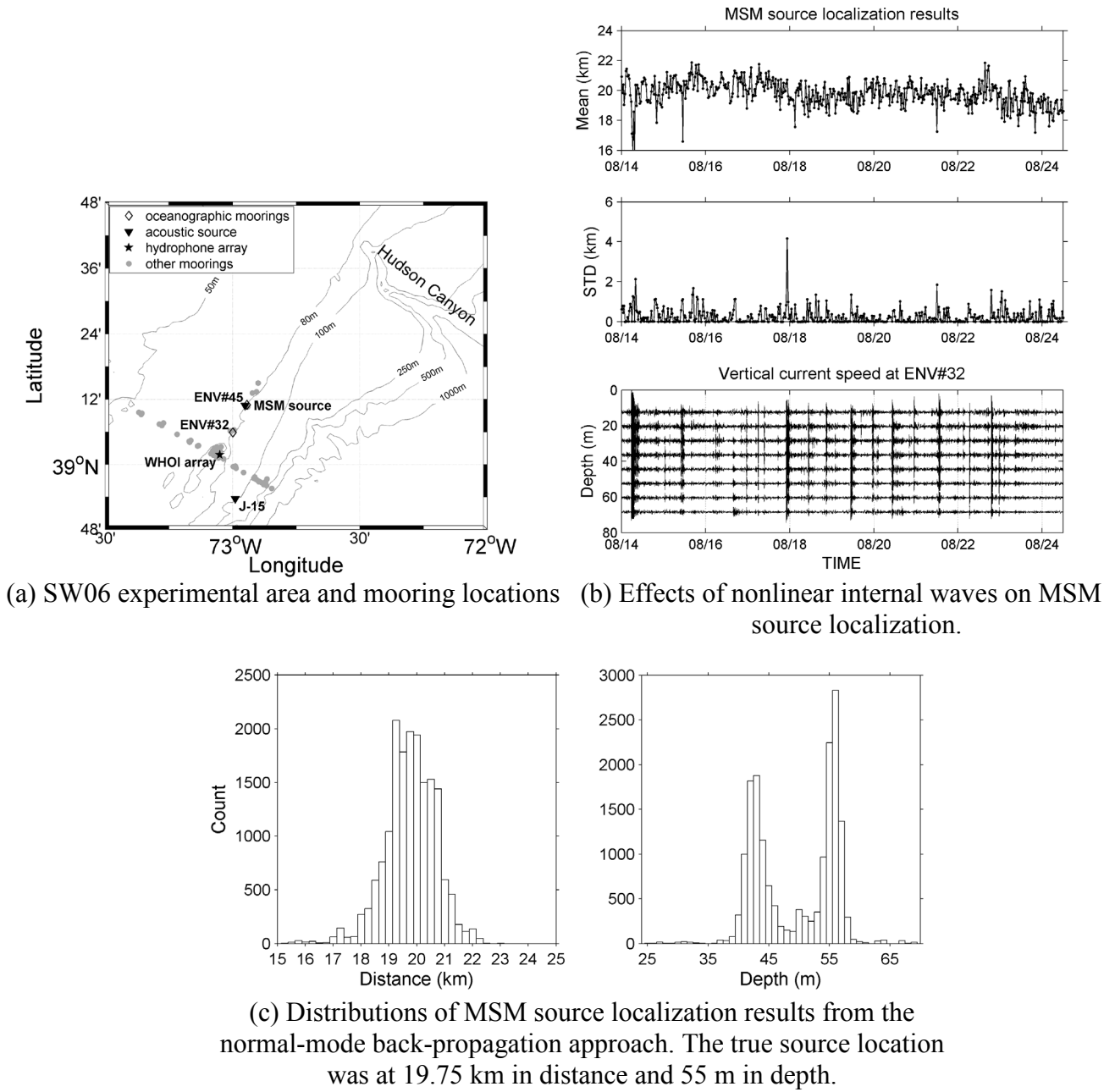(a) Vertical modes of 50 Hz sound inside and outside the internal waves



(b) Radial modes of 50 Hz sound in the internal wave duct

**Figure 5. *Whispering gallery modes in a curved nonlinear internal wave duct.***

*[ 3-D normal mode theory is used to study the whispering gallery modes occurred in a curved nonlinear internal wave duct. For each vertical mode, as shown in the panel (a), there are a set of radial modes describing the horizontal component. In this example, an internal wave duct with 25 km radius is considered. The radial modes of the second vertical mode are shown in the panel (b). One can see that the radial mode 1 humps near the outer boundary, presenting a whispering gallery mode. ]*

(a) SW06 experimental area and mooring locations

(b) Effects of nonlinear internal waves on MSM source localization.



(c) Distributions of MSM source localization results from the normal-mode back-propagation approach. The true source location was at 19.75 km in distance and 55 m in depth.

***Figure 6. Source localization using the adaptive normal-mode back-propagation method***

*[ The adaptive normal-mode back-propagation method is applied to the SW06 data. Processed signals are from one of the moored sources in the experiments, the MSM source shown in the panel (a), and the source localization results are shown in the panel (b) to correlate with the nonlinear internal wave signals measured at the environmental mooring ENV#32. A positive correlation can be seen. Distributions of the source localization results are shown in the panel (c), showing very good source range estimation. The bimodal distribution of the source depth estimates is most likely caused by unresolved mode coupling effects. ]*